International Journal of Heat and Mass Transfer 112 (2017) 972–982

Contents lists available at ScienceDirect

International Journal of Heat and Mass Transfer

journal homepage: www.elsevier.com/locate/ijhmt

Thermal management of water based SWCNTs enclosed in a partially heated trapezoidal cavity via FEM

Rizwan Ul Haq [a,*], S. Naveed Kazmi [b], Toufik Mekkaoui [c]

[a] Department of Electrical Engineering, Bahria University, Islamabad Campus, Islamabad 44000, Pakistan
[b] Department of Mathematics, Mirpur University of Science and Technology (MUST), Mirpur, Azad Kashmir, Pakistan
[c] Department of Mathematics, Faculty of Science and Technology, Errachidia, Morocco

ARTICLE INFO

Article history:
Received 20 March 2017
Received in revised form 9 May 2017
Accepted 10 May 2017

Keywords:
Natural convection
CNT–water nanofluid
Trapezoidal enclosure
Finite element method

ABSTRACT

Present study, examines the phenomena of natural convection flow in a partially heated trapezoidal cavity loaded with the nanofluid in the presence of Single Wall Carbon Nanotubes (SWCNTs). A modified model for effective thermal conductivity of carbon nanotube is used to develop the governing partial differential equations. Thermal management within the cavity is controlled via two simultaneous features: one is to use the partially heated bottom wall and other is to use conductivity of Carbon particles. Most significant and physical conditions are adjusted at the inclined walls of the trapezoidal cavity to obtain the behavior of stream lines and heat management. The Gelerkin finite element method is implemented to solve the dimensionless form of PDEs. Simulations are performed for the different lengths of the heated portion $(0.3 \leqslant L \leqslant 0.7)$, various choices of Raleigh number $(10^4 \leqslant Ra \leqslant 10^7)$ and volume fraction $(0.0 \leqslant \phi \leqslant 0.2)$. Flow field and thermal field are visualized through streamlines and isotherms. Moreover, results are obtained for Nusselt number over partially heated wall, temperature and velocity distribution over the mean position of the cavity. It is found that, by reducing the length of heated portion, flow filed is getting stronger but thermal depicts the opposite trend inside the cavity. Variation of Raleigh number also has significant influence on flow and thermal field. Conduction was dominant at low *Ra* but later on convection was found to be dominant for large choice. Fluid circulation was stronger and heat transfer rate was very slow at low viscous effects. From the graph it is clear that greater heat transfer will be occurred in the presence of nanofluid as compared to the based fluid water. Similarly velocity distribution of water is dominant as compare to the nanofluid.

1. Introduction

Heat transfer has played a vital role in numerous industrial applications. For example in vehicles and avionics, electronic equipment dissipates heat which needs cooling, heating and cooling system in buildings, industrial process, petro chemical industries, textile, food and other plants. Fluids are best source to remove, add or transfer of heat. There are several techniques has been adapted to increase heat transfer efficiency. But in some accent, way to improve the heat transfer no longer reliable, efficient and economical. Now a day efficiency of heat transfer is also improved by the augmentation of thermal conductivity of the working fluid. Suspension of the nanoparticles in a working fluid is one of the best to enhance the heat transfer. Nanofluids are studied due to their heat transfer properties. Heat transfer augmentation is an essential issue in energy saving aspects. Conventional fluids like (e.g. water, ethylene and engine oil) have low thermal conductivities than solids. For example *Cu* has thermal conductivity 700 times greater than water and 3000 time greater than engine oil. Since nanoparticles are small in size and have large specific area so nanofluids have superior properties like thermal conductivity, minimum clogging in flow passage, long-term stability and homogeneity.

Natural convection phenomena have many applications in electronic cooling, heat exchanger and double pane windows. So it is very important in engineering. Many researchers have studied convective heat transport in nanofluids. First time Khanfer et al. [1] investigated buoyancy driven heat transfer augmentation by taking 2-D heated enclosure and concluded that nanoparticles suspension increases the heat transfer rate for the given choices of Grashof number. Santra et al. [2] studied the heat transfer enhancements in a differential heating square cavity filled with *Cu*-water nanofluid using Max-well Guarnett [3] and Bruggman

* Corresponding author.
E-mail addresses: ideal_riz@hotmail.com, r.haq.qau@gmail.com (R. Ul Haq).

http://dx.doi.org/10.1016/j.ijheatmasstransfer.2017.05.041
0017-9310/

Nomenclature

C_p	specific heat, J kg^{-1} K^{-1}
g	gravitational acceleration
H	height of the trapezium cavity
k	thermal conductivity of the fluid
L	length of the trapezium cavity
Nu	Nusselt number
r	radius
p	dimensional pressure
P	dimensionless pressure
Pr	Prandtl number
Ra	Raleigh number
T^*	temperature
T	dimensionless temperature
u, v	velocity components
U, V	dimensionless velocity components
x, y	Cartesian co-ordinates
X, Y	dimensionless Cartesian components

Greek symbols

ρ_{nf}	density of nanofluid
α	thermal diffusivity
β	thermal expansion co-efficient
ϕ	volume fraction
μ	dynamic viscosity
υ	kinematic viscosity
ρ	density of the fluid

Subscripts

c	cold
h	heat
f	fluid
nf	nanofluid
CNT	Carbon nanoparticle

[4] models. Oztop and Abu Nada [5] investigated heat transfer and fluid flow due to the buoyancy forces in a partially heated enclosure loaded with different types of nanofluids and it is found that, augmentation of heat transfer at a low aspect ratio.

To see the effects of various choices of viscosity and thermal conductivity on natural convection heat transfer of Al_2O_3-water nanofluid, a study [6] was conducted. Significant enhancement of heat transfer was found to see. Ghasemi et al. [7] also conducted the study for natural convection in an enclosure loaded with Al_2O_3-water nanofluid in the presence of magnetic field. It was concluded that heat transfer rate will be increased with Raleigh number but decreased with the increasing of Hartmann number. Continuing this way Jou and Tzeng [8], Ogut [9], Das and Ohal [10], Kumar et al. [11] also gave their contributions in natural convection heat transfer in a square or rectangular enclosure.

It is not easy to study convective flow in a trapezoidal enclosure than that of square or rectangular enclosures because of sloping walls. For this purpose, Basak et al. [12] conducted numerical experiment on trapezoidal enclosure with uniform and non-uniform heating bottom wall by using Finite element method. Another investigation was conducted by Varol et al. [13,14] in trapezoidal geometry with cooled inclined wall. They used finite difference method to solve the problem. Recently, Lin and Viloi [15] and Saleh at al. [16] contributed their roles for the study of natural convection heat transfer of naofluids in vertical enclosure and trapezoidal enclosure respectively. Apart of above said studies, recently many authors investigated the study of natural convection flow of nanofluid for various shapes of cavity [17–20].

Despite all these existing efforts done by the researchers, there is still a lack of information relevant to the heat transfer augmentation in trapezium enclosure loaded with nanofluids with respect to the partially heated domain. The purpose of the present article is to investigate numerically the natural convection heat transfer in a trapezoidal enclosure loaded with Cu-water nanofluids with different configuration and boundary conditions that are not discussed so far. The top wall is insulated while the bottom wall is partially heated. Both inclined side walls are kept cold. Flow field and thermal field are visualized for different lengths of the heated portion, various choices of Raleigh numbers and volume fraction. Heat transfer performance is observed through Nusselt number. Temperature and velocity distribution over the mean position are also calculated (see Fig. 1)

2. Mathematical formulation

2.1. Physical problem

The objective of the present paper is to examine the natural convection flow and heat transfer inside the trapezium enclosure loaded with CNT-water nanofluid. For this purpose the bottom wall of the cavity in computational trapezium domain with length L is placed at the origin of the Cartesian co-ordinate system. The enclosure is filled with CNT-water nanofluid. The top wall is insulated while the bottom wall is partially heated. Both inclined walls are kept cold. Buoyancy forces owing to the differential heating are acting on the fluid. Heat transfer due to the natural convection is taken into account. Simulations are performed for various lengths of the heated portion ($0.3 \leqslant L \leqslant 0.7$), various choices of Raleigh number ($10^4 \leqslant Ra \leqslant 10^7$) and volume fractions ($0 \leqslant \phi \leqslant 0.2$). The aim was to observe heat augmentation and heat transfer rate. The flow and thermal fields are visualized in the forms of streamlines and isotherms. All physical properties of the working fluid were supposed to be constant except density difference in the body force term under Boussinesq assumption. The dissipation effect is neglected.

2.2. Boundary conditions

For the left and right inclined walls $T^* = T_c$

For the partially heated bottom wall $\begin{cases} \frac{\partial T^*}{\partial y} = 0 & x < L \\ T^* = T_h & at\ L \\ \frac{\partial T^*}{\partial y} = 0 & x > L \end{cases}$

For the top insulated wall $\frac{\partial T^*}{\partial y} = 0$

At all solid boundaries $u = v = 0$

2.3. Governing equations

For the present study a steady, incompressible, laminar, non-viscous two-dimensional flow is taken into account. The gravitational force is acting vertically downward. The radiation and dissipation effects are neglected. The governing equation under Boussinesq approximation are given below

$$\frac{\partial u}{\partial x} + \frac{\partial v}{\partial y} = 0, \tag{1}$$

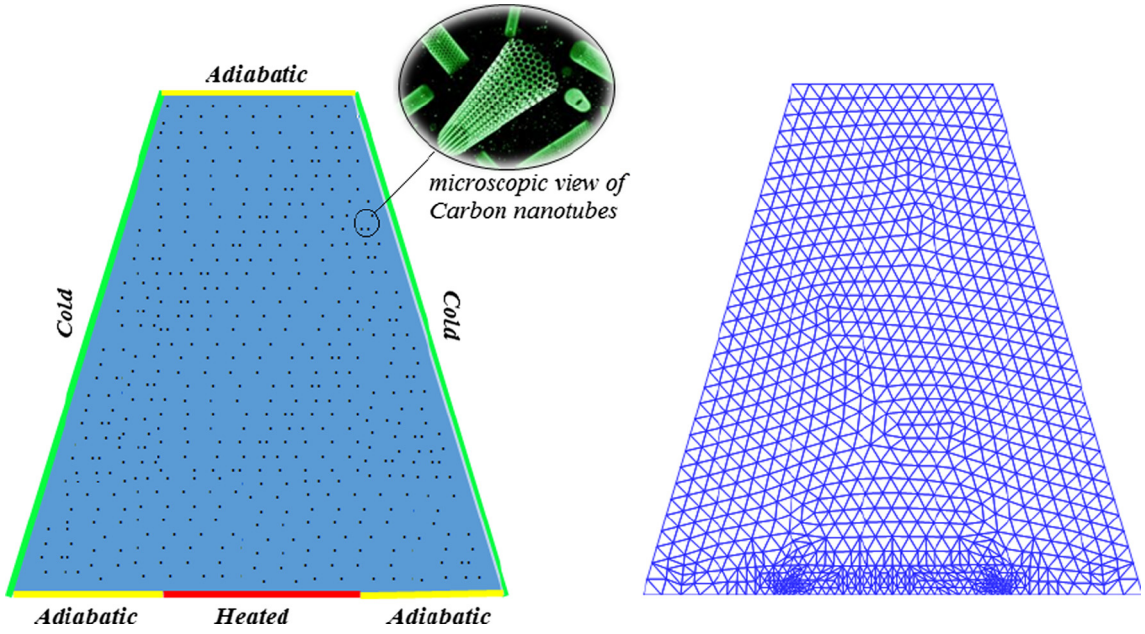

Fig. 1. Geometry of the trapezoidal cavity and computational domain of the model.

$$\rho_{nf}\left(u\frac{\partial u}{\partial t}+v\frac{\partial u}{\partial r}\right)=-\frac{\partial p}{\partial x}+\mu_{nf}\left(\frac{\partial^2 u}{\partial x^2}+\frac{\partial^2 u}{\partial y^2}\right), \tag{2}$$

$$\rho_{nf}\left(u\frac{\partial v}{\partial x}+v\frac{\partial v}{\partial y}\right)=-\frac{\partial p}{\partial y}+\mu_{nf}\left(\frac{\partial^2 v}{\partial x^2}+\frac{\partial^2 v}{\partial y^2}\right)-g\rho_{nf}\beta_{nf}(T^*-Tc), \tag{3}$$

$$\left(u\frac{\partial T^*}{\partial x}+v\frac{\partial T^*}{\partial y}\right)=\alpha_{nf}\left(\frac{\partial^2 T^*}{\partial x^2}+\frac{\partial^2 T^*}{\partial y^2}\right). \tag{4}$$

In the above system of equations, u and v are velocities along $x-$ and $y-$ directions, respectively. T^* is the temperature and P is the pressure. The terms heat capacity, thermal expansion coefficient and density of nanofluid is defined as:

$$\left.\begin{aligned}(\rho C)_{nf}&=(1-\phi)(\rho C)_f+\phi(\rho C)_p,\\ \beta_{nf}&=(1-\phi)\beta_{f+}\phi\beta_p,\\ \rho_{nf}&=(1-\phi)\rho_f+\phi\rho_p,\end{aligned}\right\} \tag{5a}$$

New effective thermal conductivity purposed by Thang et. al. [21]:

$$\frac{k_{nf}}{k_f}=1+\frac{1}{3}\frac{k_{CNT}\phi r_f}{k_f(1-\phi)r_{CNT}}, \tag{5b}$$

where r is the radius (for CNT $r_{CNT}=10$ nm and for water molecule $r_f=0.1$ nm). Effective dynamic viscosity of the nanofluid Maxwell-Garnett Models is

$$\mu_{nf}=\frac{\mu_f}{(1-\phi)^{2.5}}, \tag{5c}$$

The dimensionless quantities are:

$$X=\frac{x}{L},\quad Y=\frac{y}{L},\quad U=\frac{uL}{\alpha_f},\quad V=\frac{vL}{\alpha_f},\quad T=\frac{T^*-T_c}{T_h-T_c},\quad P=\frac{pL^2}{\rho_f\alpha_f^2},$$

$$v_f=\frac{\mu_f}{\rho_f},\quad Pr=\frac{v_f}{\alpha_f},\quad Ra=\frac{\beta_f(T_h-T_c)L^3}{\upsilon_f\alpha_f}.$$

Table 1
Thermophysical properties of water and SWCNTs.

Thermo-Physical properties	Water	SWCNTs
Cp	4179	425
ρ	997.1	2600
k	0.613	6600
β	21×10^5	0.33×10^5
r	0.1	10

where Ra, Pr denote Rayleigh number and Prandtl number, respectively. Dimensionless form of the Eqs. (1)–(4) by is given by:

$$\left(U\frac{\partial U}{\partial X}+V\frac{\partial U}{\partial Y}\right)=-\frac{\rho_f}{\rho_{nf}}\left(\frac{\partial P}{\partial X}\right)+Pr\frac{v_{nf}}{v_f}\left(\frac{\partial^2 U}{\partial X^2}+\frac{\partial^2 U}{\partial Y^2}\right), \tag{6}$$

$$\left(U\frac{\partial V}{\partial X}+V\frac{\partial V}{\partial Y}\right)=-\frac{\rho_f}{\rho_{nf}}\left(\frac{\partial P}{\partial Y}\right)+Pr\frac{v_{nf}}{v_f}\left(\frac{\partial^2 V}{\partial X^2}+\frac{\partial^2 V}{\partial Y^2}\right)-\frac{(1-\phi)\rho_f\beta_f+\phi\rho_{CNT}\beta_p}{\rho_{nf}\beta_f}RaPrT, \tag{7}$$

$$\left(U\frac{\partial T}{\partial X}+V\frac{\partial T}{\partial Y}\right)=\frac{\alpha_{nf}}{\alpha_f}\left(\frac{\partial^2 T}{\partial X^2}+\frac{\partial^2 T}{\partial Y^2}\right). \tag{8}$$

In the above equations, $Pr=\frac{v_f}{\alpha_f}$ is the Prandtl number and $Ra=\frac{g\beta_f(T_h-T_c)L^3}{v_f\alpha_f}$ is the Rayleigh number. Boundary conditions within the bounded domain as defined as:

At the left and right inclined walls $T=0,$ (9a)

At the top wall $\frac{\partial T}{\partial Y}=0,$ (9b)

At the partially heated wall $\begin{cases}\frac{\partial T}{\partial Y}=0, & X<L,\\ T=1, & at\ L,\\ \frac{\partial T}{\partial Y}=0. & X>L,\end{cases}$ (9c)

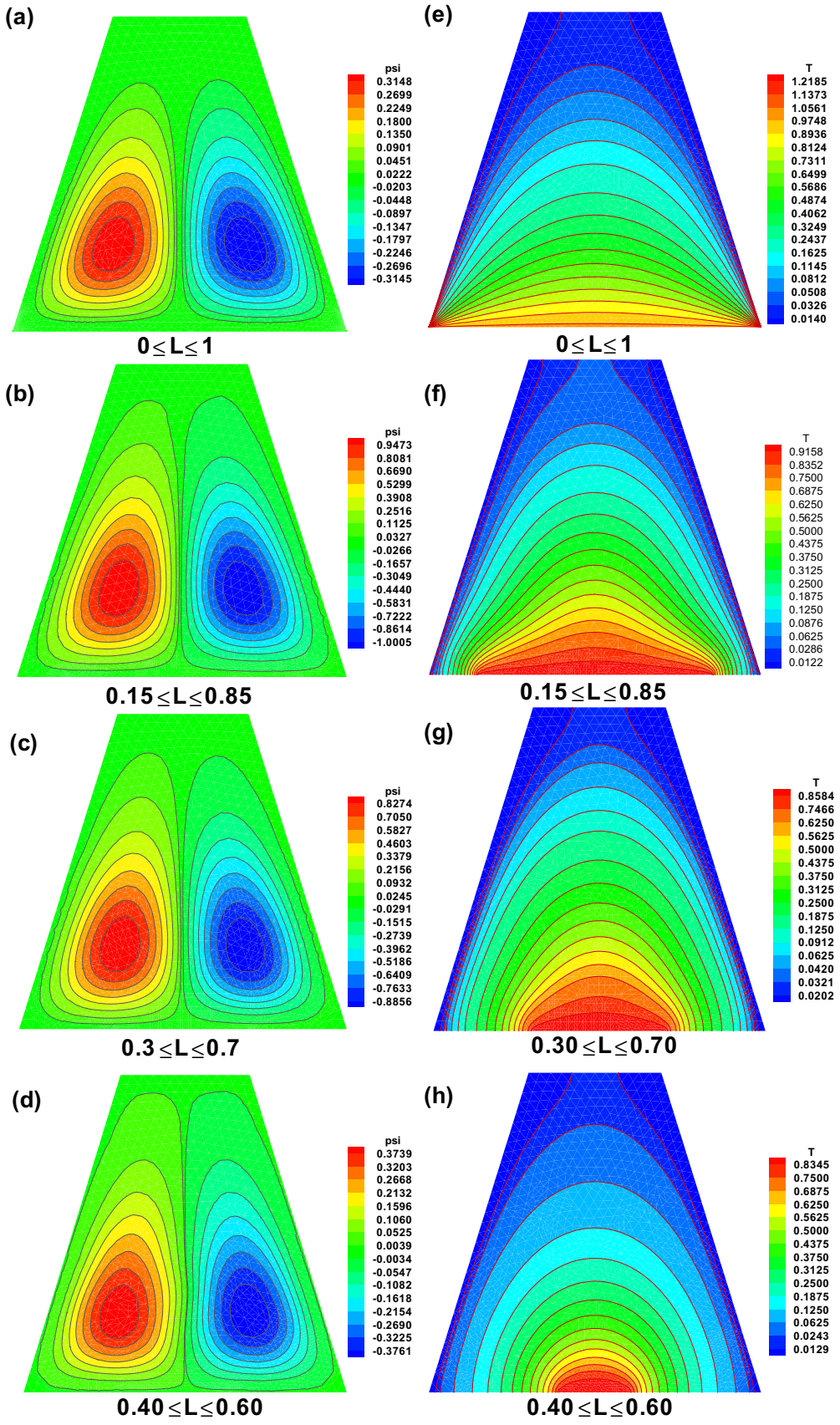

Fig. 2. Variation of streamlines and isotherms for various partially heated domains when $Ra = 10^4, \phi = 0$.

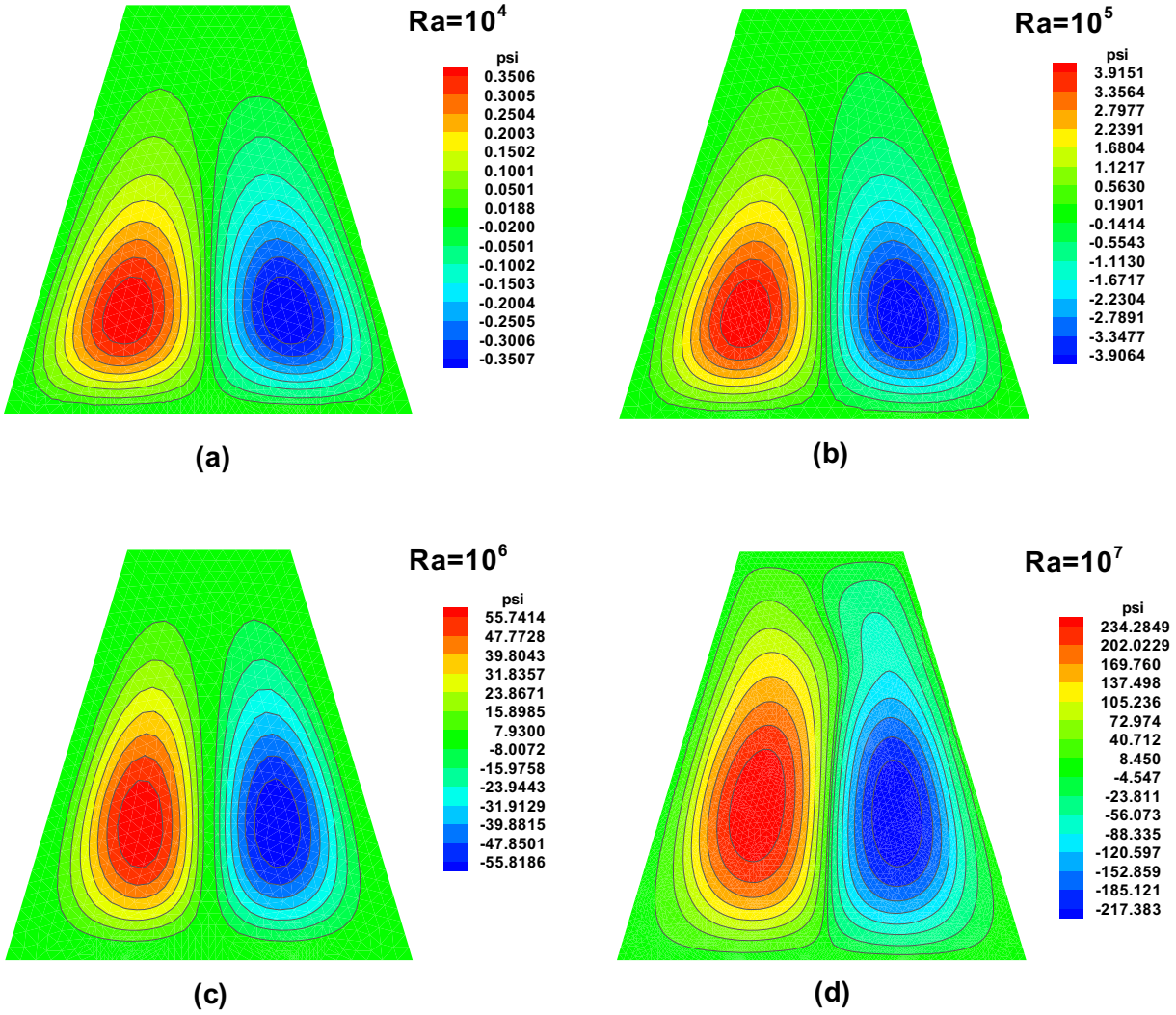

Fig. 3. Variation of streamlines for various values of Rayleigh number (a) $Ra = 10^4$, (b) $Ra = 10^5$, (c) $Ra = 10^6$, (d) $Ra = 10^7$ when $\phi = 0.2$.

At all solid boundaries $U = V = 0$. (9d)

Average Nusselt number along a partially heated domain of enclosure is defined as:

$$Nu_{avg} = \int_L -\frac{knf}{kf}\frac{dT}{dY}dX. \tag{10}$$

where L is partially heated domain that is: $L = \{(X, Y) \in \mathbb{R}^2 | 0 \leqslant X \leqslant 1 \wedge Y = 0\}$.

3. Solution of the problem

In order to deal this complex nature model, Finite Element Method (FEM) is used along with the Galerkin weigh residue approach to solve Eqs. (6)–(8) along with the boundary conditions (9a)–(9d). To solve the system of nonlinear equations, solution domain is discretized via finite number of elements and then non-uniform elements are generated at partially heated domain. A grid sensitivity test is made for various elements and found better for accurate results. Further detail of the method is described in by Taylor and Hood [22] and Dechaumphai [23]. The pressure term (P) is eliminated via continuity equation using the constraint equation $P = -\gamma(\frac{\partial U}{\partial X} + \frac{\partial V}{\partial Y})$. The continuity Eq. (1) satisfied for large values of $\gamma = 10^7$. By replacing the pressure P, terms in Eqs. (6) and (7) we get:

$$\left(U\frac{\partial U}{\partial X} + V\frac{\partial U}{\partial Y}\right) = \gamma\frac{\rho_f}{\rho_{nf}}\frac{\partial}{\partial X}\left(\frac{\partial U}{\partial X} + \frac{\partial V}{\partial Y}\right) + Pr\frac{\nu_{nf}}{\nu_f}\left(\frac{\partial^2 U}{\partial X^2} + \frac{\partial^2 U}{\partial Y^2}\right), \tag{11}$$

and

$$\left(U\frac{\partial V}{\partial X} + V\frac{\partial V}{\partial Y}\right) = \gamma\frac{\rho_f}{\rho_{nf}}\frac{\partial}{\partial Y}\left(\frac{\partial U}{\partial X} + \frac{\partial V}{\partial Y}\right) + Pr\frac{\nu_{nf}}{\nu_f}\left(\frac{\partial^2 V}{\partial X^2} + \frac{\partial^2 V}{\partial Y^2}\right) - \frac{(1-\phi)\rho_f\beta_f + \phi\rho_{CNT}\beta_p}{\rho_{nf}\beta_f}RaPrT, \tag{12}$$

The steps involved in the finite element analysis are as follows:

(a) Discretization of the domain into elements.
(b) Derivation of element equations.
(c) Assembly of Element Equations.
(d) Imposition of boundary conditions.
(e) Solution of assembled equations.

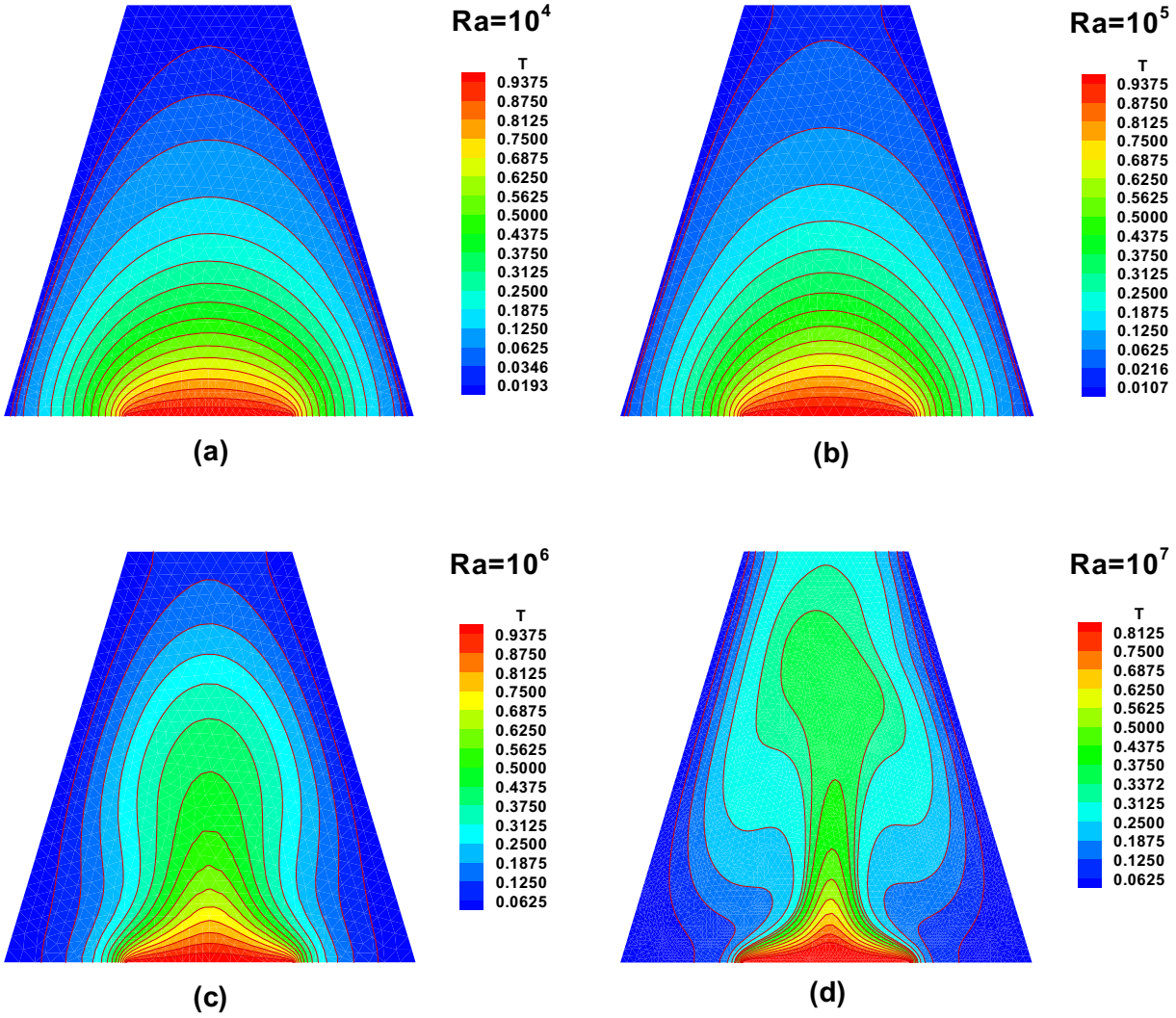

Fig. 4. Variation of isotherms for various values of Rayleigh number (a) $Ra = 10^4$, (b) $Ra = 10^5$, (c) $Ra = 10^6$, (d) $Ra = 10^7$ when $\phi = 0.2$.

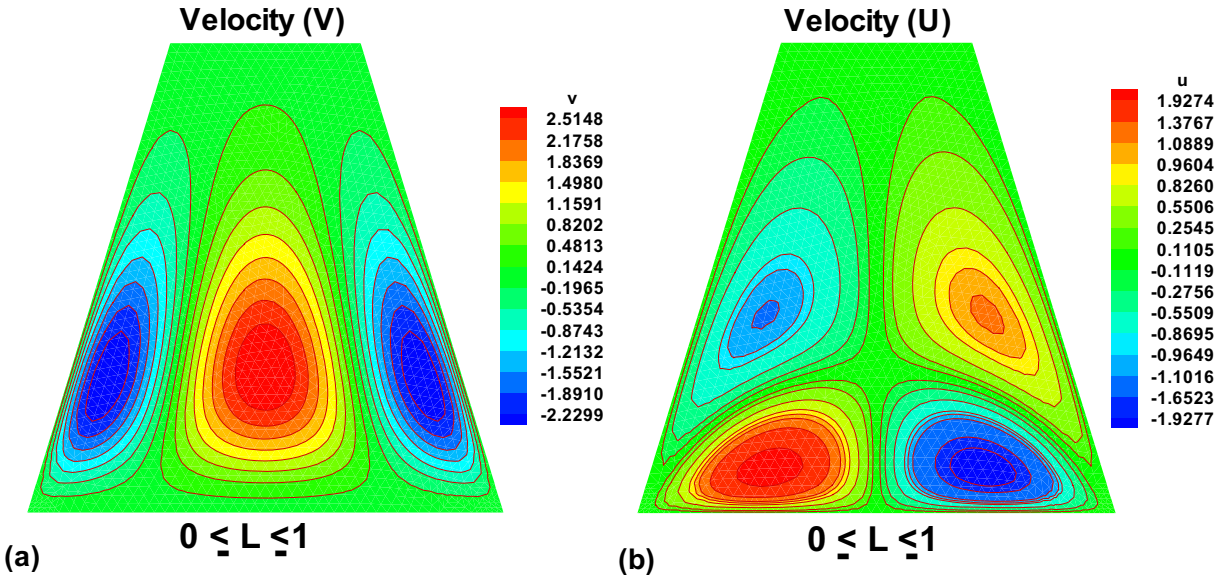

Fig. 5. Variation of (a) velocity V and (b) velocity U when $Ra = 10^4, \phi = 0.2$.

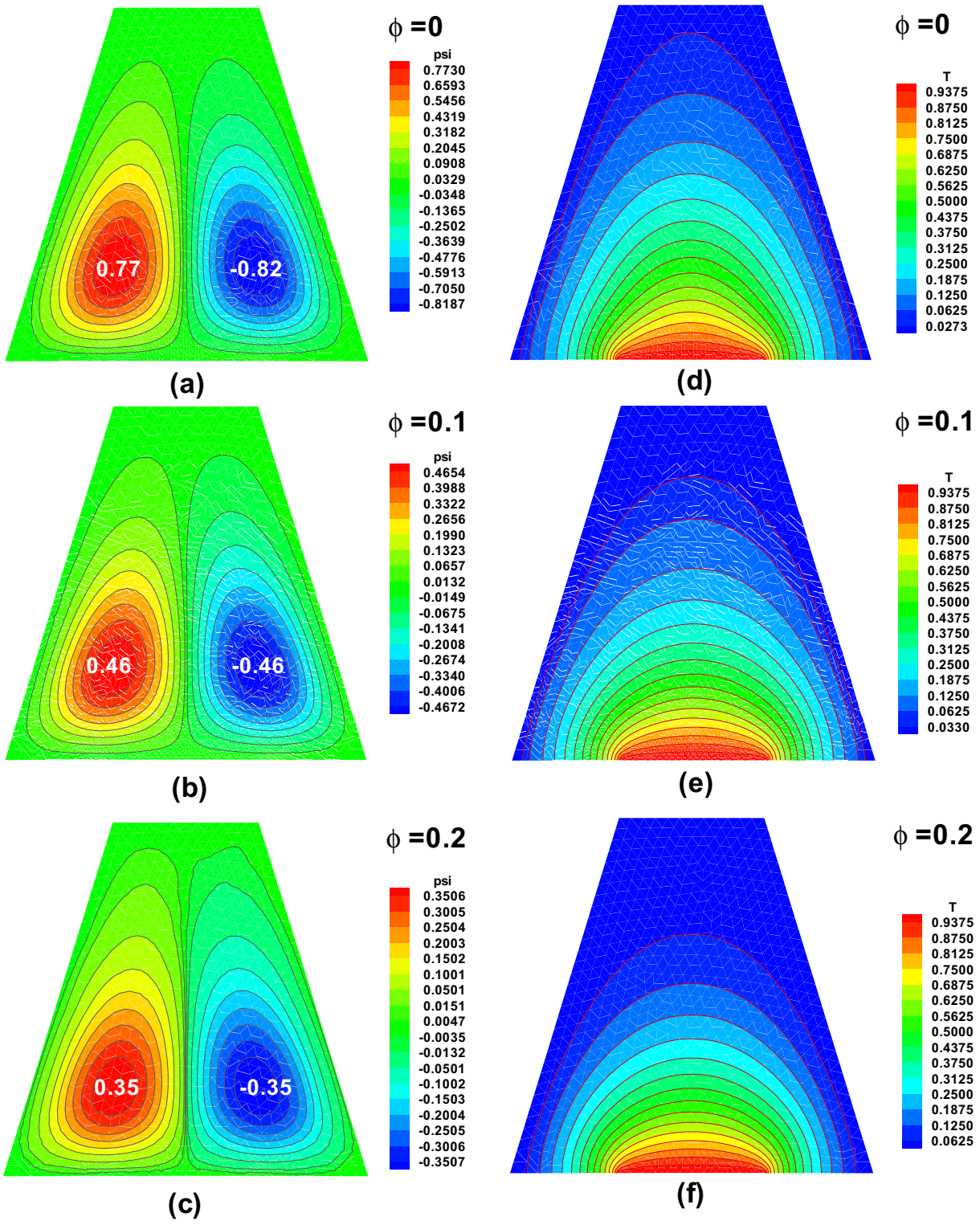

Fig. 6. Variation of streamlines for (a) $\phi = 0$, (b) $\phi = 0.1$, (c) $\phi = 0.2$ and variation of isotherms for (d) $\phi = 0$, (e) $\phi = 0.1$, (f) $\phi = 0.2$ when $Ra = 10^4$.

4. Results and discussion

In order to determine the paths or the trajectories traced by the fluid's molecules, we have used the stream function to obtain the stream lines. Similarly, temperature distribution within the restricted domain of the cavity is obtained via isotherms. As it is mentioned earlier that bottom wall of trapezoidal cavity is conserved to be partially heated. So entire produced results describe the variation of isotherms for partially heated domain $0.3 \leqslant L \leqslant 0.7$ of length 0.4 unit along the x-axis. Throughout in the computations Prandtl number $(Pr = 6.2)$is kept fixed for the based fluid. Thermophysical properties of both water and CNTs are defined in Table. 1.

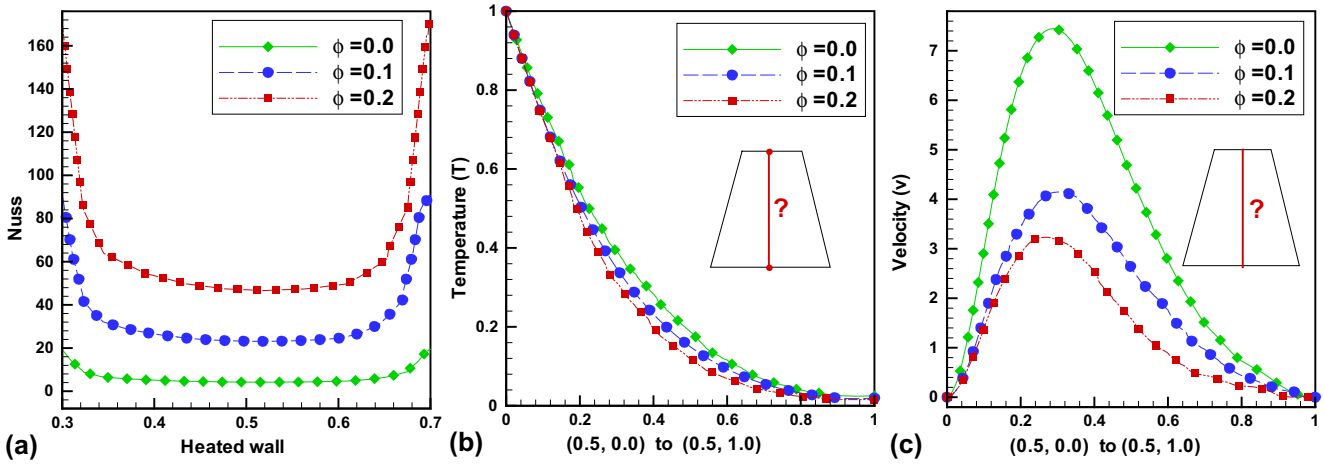

Fig. 7. Variation of (a) Nusselt number along $0.3 \leqslant L \leqslant 0.7$, (b) temperature T and (b) velocity V along mean position of cavity from $(0.5, 0)$ to $(0.5, 1)$.

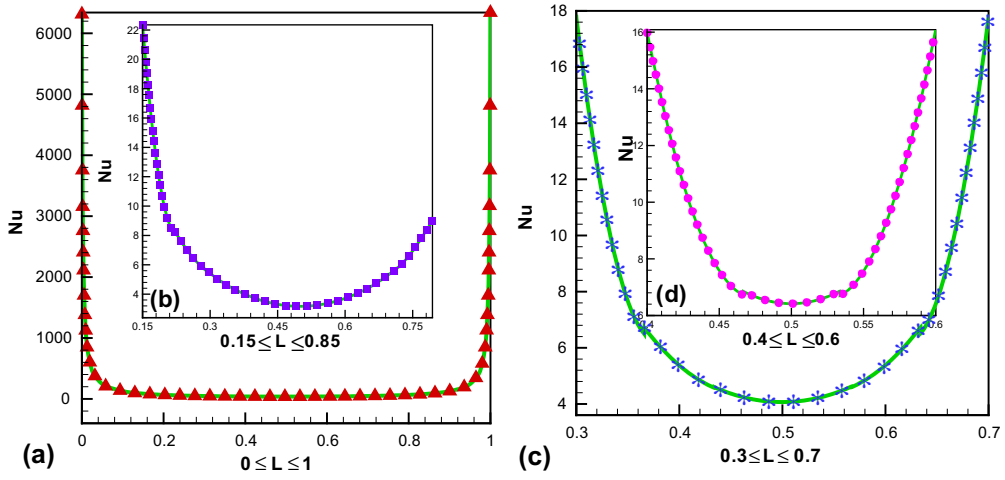

Fig. 8. Variation of Nusselt number along (a) $0 \leqslant L \leqslant 1$, (b) $0.15 \leqslant L \leqslant 0.85$, (c) $0.3 \leqslant L \leqslant 0.7$, (d)$0.3 \leqslant L \leqslant 0.7$.

4.1. Effects of partially heated domain

Fig. 2(a)–(d) describes the behavior of streamlines with respect to different partially heated bottom wall. Symmetric behavior of streamlines is obtained for each partially heated domain having line of symmetry is $x = 0.5$. Fig. 2 is plotted for the fix values of Raleigh number $Ra = 10^4$ and nanoparticle volume fraction $\phi = 0$. Since both inclined walls are kept cold so fluid rises up owing to the differential heating and falls down along the sides inclined walls. Thus fluid's molecules distributes in two symmetric bullous. From Fig. 2(a)–(d) it can be seen that the symmetry of these bullous do not break up for all different lengths of heated portions. However as length is decreasing these rotating bullous are increasing and occupying most part of the trapezium enclosure. Fluid flow is getting stronger with respect to the decreasing lengths of heated portion because of natural convection.

Fig. 2(e)–(h) illustrates the behavior of heat flow via isotherms with respect to the different partially heated domain of the bottom wall. In Fig. 2(e), the smooth lines of the isotherms depict the life span of heat transferring inside the cavity. Thermal boundary layers are found to grow from the edges of the heated bottom wall. Since fluid remains cooler near the side cold walls due to less mobility of the fluid and consequently thermal layers become thick at the upper part of the cavity. So conduction will take place in the significant region. Fig. 2(f)–(h) shows that as length of the heated bottom is decreasing then thermal boundary layers are growing only from the heated portion and length of the heat transfer is becoming less. Most amount of the fluid becoming cooler near the side walls and top wall. Uniform isotherms indicate strong conduction is dominant in the bounded domain.

4.2. Effects of Raleigh number

The Fig. 3(a)–(d) represents the streamlines of SWCNT-water nanofluid for the wide range of Raleigh number $Ra = 10^4$ to $Ra = 10^7$. The flow forms two symmetric bullous along the inclined walls which is due to the boundary conditions. Raleigh number associates with the buoyancy driven flow (i.e. natural convection). It is evident from Fig. 3(a) that at low value of $Ra = 10^4$, magnitudes of the ψ is small that represent the conductive heat transfer inside an enclosure. Moreover the diameter of the right bullous is relatively small to the left one due to the less fluid mobility. Overall flow pattern shows that viscosity effect of nanofluid is dominant for low Raleigh number. While, there is an insignificant changes on flow pattern at $Ra = 10^5$. This time diameter of the left bullous is less than the right one. Once again conduction is dominant. At high Raleigh number $Ra = 10^6$, these rotating cells are appeared

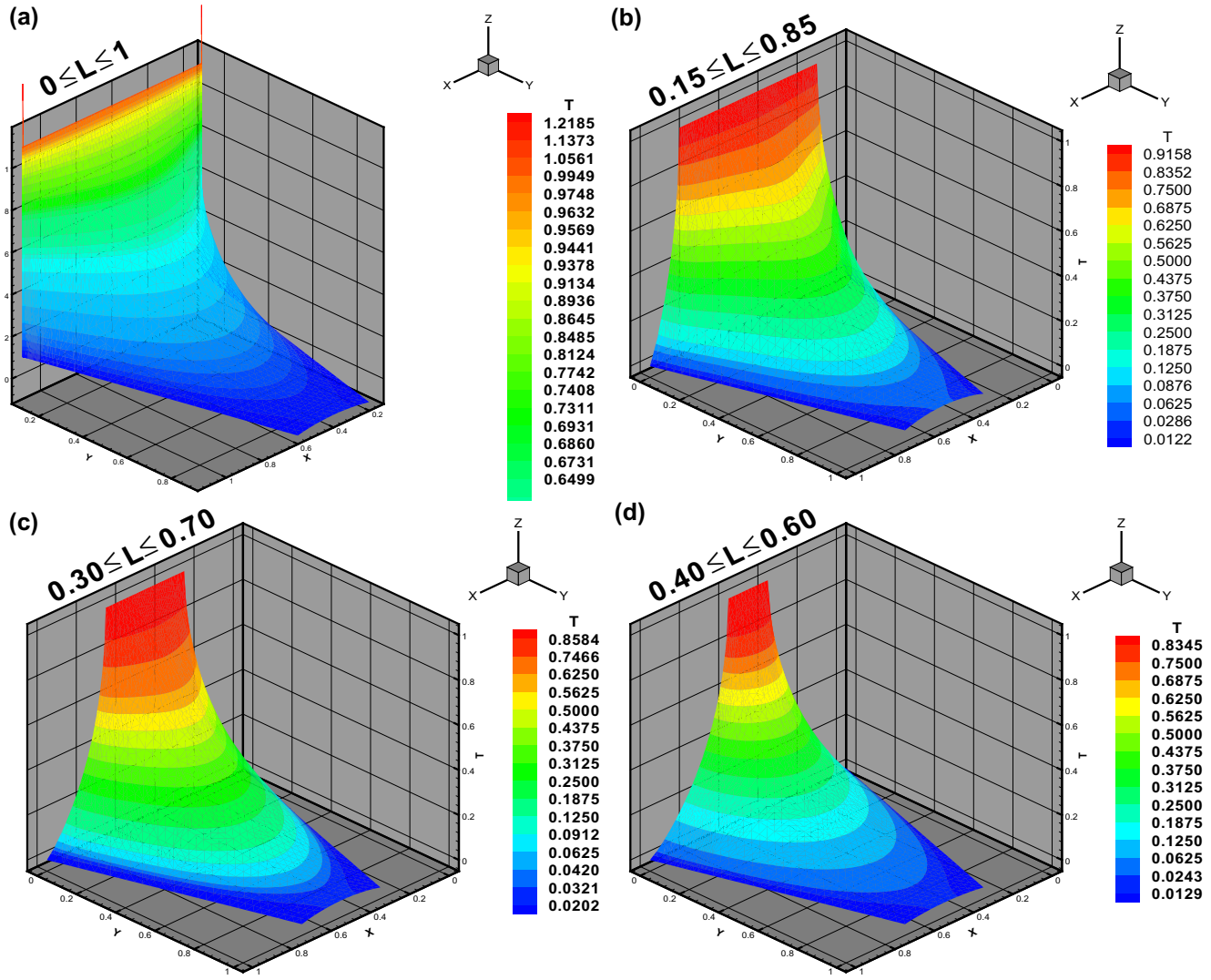

Fig. 9. Three dimensional view of isotherms for various partially heated domain (a) $0 \leqslant L \leqslant 1$, (b) $0.15 \leqslant L \leqslant 0.85$, (c) $0.15 \leqslant L \leqslant 0.85$, (d) $0.40 \leqslant L \leqslant 0.60$.

at the upper part but with low deviation between them. Actually fluid rises in the middle part of the enclosure due to the increasing effect of the dominant buoyant driven forces to the viscous effect of nanofluid at high Raleigh number. Convective heat flow is found to be dominant. From (d), at a large value of $Ra = 10^7$ these symmetric rolls occupy the most part of the trapezium enclosure and the core of the cells are increased due to the high convection and mobility of the fluid. Consequently, this way to produce the motion gives strengthens in the circulation. Absolute value of stream function $|\psi|$ attains its maximum values 0.35, 3.9, 55.74 and 234.2 for the corresponding values of Ra at $10^4, 10^5, 10^6$ and 10^7 respectively.

Fig. 4(a)–(d) illustrates isotherms for the vide choices of Rayleigh number ($10^4 \leqslant Ra \leqslant 10^7$). It is clear from the plots (a) that for small values of $Ra = 10^4$, counters of isotherms are smooth lines which tell the time length of heat transferring. Thermal boundary layers seem to grow from the bottom heated portion and becoming thick uniformly at the upper part of the enclosure. Which indicates conduction is dominant in the whole domain. Slow motion of fluid's molecules it is found due to low Rayleigh number, so large amount of the fluid's molecules will remain cooler near to the cold sides of the walls. This phenomenon will create thickness in thermal boundary layer at the top middle part of enclosure. This situation remains same for $Ra = 10^5$. However, when $Ra = 10^6$ then viscosity effects the nanofluid becomes less to the fluid motion due to the dominating buoyant forces. So thermal layers are dispersed and found to be non-uniform shape. This shows that this phenomenon arises due to convection. At maximum value of Rayleigh number, thermal boundary layer is thick near the side walls due the strong effect of buoyancy forces. Overall convection is dominant throughout the enclosure. Common to all cases temperature θ is high at the heated portion and gradually decreasing as fluid moves towards the side cold walls and upper part of the enclosure.

4.3. Effects of nanoparticle volume fraction

To govern the behavior of the velocities, results are plotted for U and V for fully heated domain ($0 \leqslant L \leqslant 1$) when $Ra = 10^4$. One can observe the symmetric behavior of the bolus for each velocity profile plotted in Fig. 5(a) and (b). For velocity V, maximum influence of the fluid is found in vertical direction however behavior of U is influential in the whole domain of the cavity.

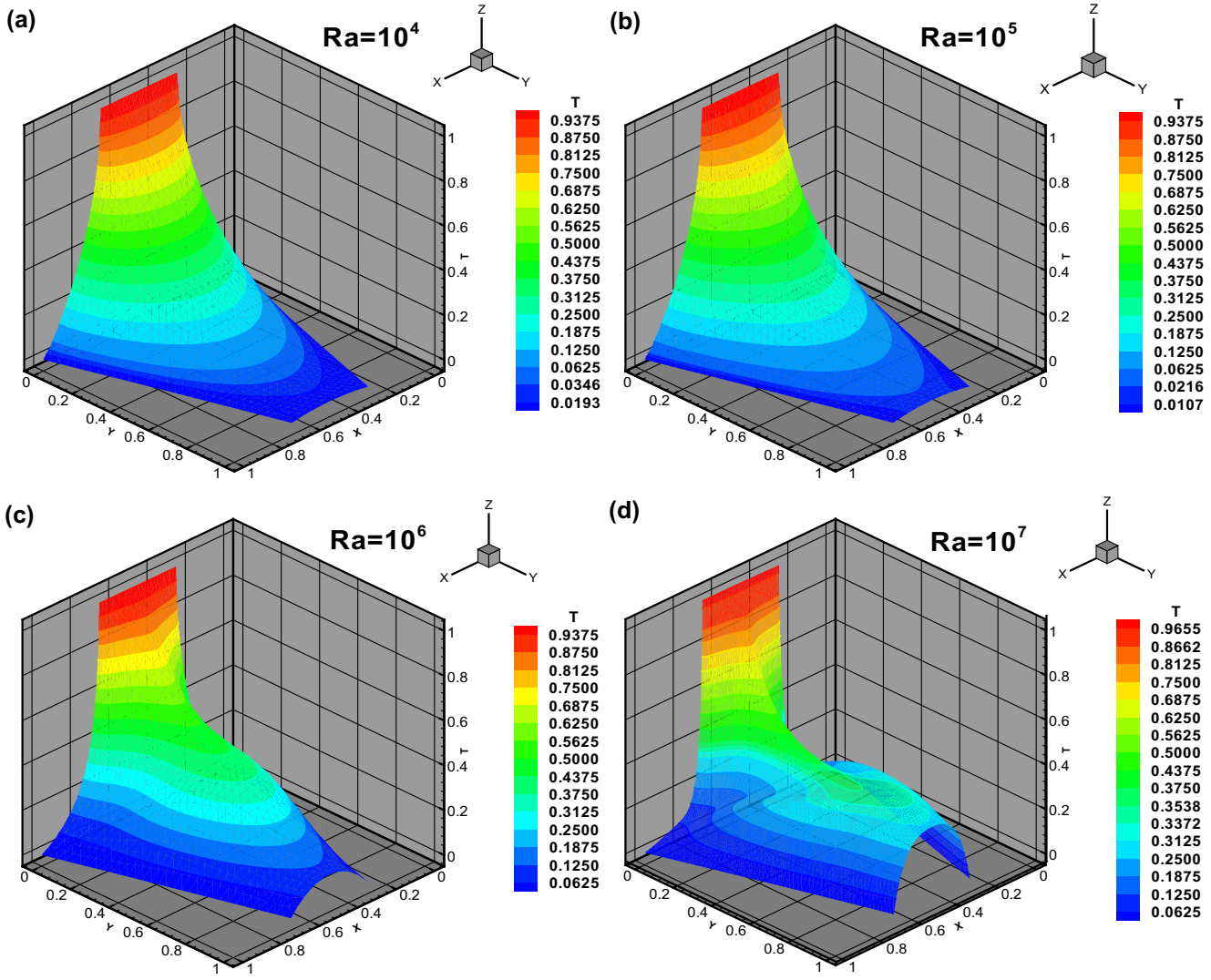

Fig. 10. Three dimensional view of isotherms for various values of Rayleigh number (a) $Ra = 10^4$, (b) $Ra = 10^5$, (c) $Ra = 10^6$, (d) $Ra = 10^7$ when $0.3 \leqslant L \leqslant 0.7$.

Fig. 6(a)–(c) represents the streamline for the case of water $\phi = 0.0$ and nanofluids $\phi = 0.1$ and 0.2. While Rayleigh number $(Ra = 10^4)$ for the partially heated domain is $0.3 \leqslant L \leqslant 0.7$ of length 0.4 is kept fixed. At small values of Rayleigh number, magnitudes of stream functions are small that indicates the conductive heat transfer is dominant for water and nanofluids. Flow pattern contains two symmetric circulating rolls inside the cavity because of the boundary conditions. Flow pattern is qualitatively similar for all cases of water $\phi = 0.0$ and nanofluids $\phi = 0.1$ and 0.2. It is mentioned earlier, viscous effects are dominant at low Rayleigh number. So, the central smallest bolus size for water $(\phi = 0)$ is bigger than that of nanofluid i.e., the bolus size corresponding to $|\psi| = 0.82$ for $\phi = 0$ is bigger than the bolus sizes corresponding to $|\psi| = 0.46$ and 0.35 for $\phi = 0.1$ and 0.2, respectively. Clearly as ϕ is increasing intensity of the circulation flow is becoming less. Thus the flow intensity remains stronger for the water as compared to the nanofluid.

Fig. 6(d)–(f) describes the isotherms for the case of water $\phi = 0$ and the nanofluid with nanoparticle volume fraction $\phi = 0.1$ and 0.2. While Rayleigh number $(Ra = 10^4)$ for the partially heated domain is $0.3 \leqslant L \leqslant 0.7$ of length 0.4 is kept fixed. The qualitative pattern of the isotherms remain same for all cases of ϕ. Thermal layers are growing from the bottom heated wall except the life span of the temperature contours is found more for low viscosity $\phi = 0$. Note that thermal boundary layers are thick and occur on the entire cavity for the water and are confined to only middle portion for the nanofluid due to the increasing viscosity effect and less mobility fluid. So the amount of the warmer fluid will become less than the cooler part as viscosity will be increased.

4.4. Effects of nanoparticle volume fraction and partially heated domain on Nusselt number, temperature and velocity

Fig. 7(a)–(c) illustrates the variation of Nusselt number over the heated bottom wall, temperature and velocity distribution along mean position of the cavity from (0.5, 0.0) to (0.5, 1.0) for solid volume fractions $\phi = 0.0, 0.1$ and 0.2. The heat transfer performance inside an enclosure is visualized in terms of Nusselt number and temperature while the fluid motion is visualized with the help of velocity profile. Green, blue and red dotted lines are used for $\phi = 0.0, 0.1$ and 0.2 respectively. From Fig. 7(a), it is clear that all plots have same trends on distribution of Nusselt numbers for nanofluid and water. Nusselt number is found largest for $\phi = 0.2$ and smaller for water which is due to the fact of higher thermal

conductivity of nanofluid than water. So as ϕ is increasing, the Nusselt number is also increasing which is a sign of great heat transfer in the enclosure in the presence of nanofluid. Similarly, Fig. 7(b) represents the variation of temperature T inside the trapezium enclosure versus mean position (distance of y-axis) for the case of water $\phi = 0$ and nanofluids $\phi = 0.1$ and 0.2. For all cases of $\phi = 0, 0.1$ and 0.2 temperature T attains maximum value 1 at initial point of the mean position and monotonically decreasing until it attains the minimum value 0 at end point of mean position. Moreover when volume fraction $\phi = 0.0$ temperature decreases gradually but $\phi = 0.2$ it decrease rapidly. Fig. 7(c) represents the velocity distribution of water and nanofluids versus mean position of the enclosure (distance of y-axis). Velocity exhibits parallel trends for water and nanofluids. Less velocity is obtained at the initial and final points of the mean position. For nanofliuds $\phi = 0.1$ and 0.2 the velocities are monotonically increasing and decreasing before and after that point 0.3. But for water $\phi = 0.0$, velocity rapidly increases and decreases before and after 0.3. This is because nanofluids become less dense as compared to water. So velocity of the working fluid is higher than that of nanofluid.

Variation of Nusselt number at different partially heated portion is measured in Fig. 8(a)–(d). One can observe that heat transfer rate is depending upon the length of bottom heated surface. When heated domain of length $0 \leqslant L \leqslant 1$, then maximum value of Nusselt number is obtained and variation of Nusselt number is gradually decreases as we decrease the length of heated domain.

4.5. 3-D behaviors of isotherms for various partially heated domain and Rayleigh number

As we have discussed earlier, partially heated domain significantly affects the restricted domain of the nanofluid enclosed in a trapezoidal cavity. In Fig. 9(a)–(d), results demonstrate the three dimensional view of isotherms when bottom wall of the cavity is heated from different length. In Fig. 9(a), one can observe that maximum value of T is about 1.2186 for fully heat bottom wall of the cavity. And similarly, when the heated length is $0.15 \leqslant L \leqslant 0.85$ then maximum temperature distribution is about 0.9158 (see Fig. 9(b)). So gradually, this ration of temperature variation will decrease as we decrease the heated length of the cavity (see Fig. 9(c) and (d)).

Fig. 10(a)–(d) depicts the three dimensional variation of isotherms for various values of Rayleigh number. One can observe that thermal boundary layers increases from the bottom heated portion and becoming thick uniformly at the upper part of the enclosure. This phenomenon indicates that conduction is dominant in the restricted domain of the cavity. As we have discussed earlier that, less fluid motion is obtained at low Rayleigh number and so large amount of the fluid's molecules will remain cooler near to the cold side's walls. Due to this fact this phenomenon will create thickness in thermal boundary layer at the top middle part of enclosure. However this behavior remains same for $Ra = 10^5$. When we increase the value of Rayleigh number $Ra = 10^6$ then viscosity effects the nanofluid becomes less to the fluid motion due to the dominating buoyant forces. Overall convection is dominant throughout the enclosure.

5. Conclusions

The purpose of this study is to analyze the numerical simulation of natural convection in a trapezoidal enclosure loaded with CNT-water nanofluid for different lengths of heated portion with the help of Finite Element method. By considering wide range of Raleigh number and different choices of solid volume fraction of nanoparticles results are computed graphically. The graphs were also made for the distributions of Nusselt number over partially heated bottom wall, temperature and velocity inside the cavity. The conclusion drawn from this investigation is: the flow field was found stronger but thermal filed had opposite behavior on decreasing the length of heated portion. When *Ra* number was increased both flow and thermal fields were found stronger. Conduction seemed dominant at low *Ra* and convection dominant for large choices. Fluid rotation became stronger and heat transfer rate was very slow at low viscous effects. From the graph it was observed that greater heat transfer occurred in the presence of nanofluids as compared to water. Similarly velocity of the water is more than that of nanofluid.

References

[1] K. Khanfer, K. Vafai, M. Lightstone, Bouyancy-driven heat transfer enhancement in two-dimensional enclosure utilizing nanofluid, Int. J. Heat Mass Transfer 46 (2003) 3639–3653.
[2] A.K. Santra, S. Sen, N. Chakraborty, Study of heat transfer characteristics of copper-water nanofluid in a differentially heated square cavity with different viscosity models, J. Enhancement Heat Transfer 15 (4) (2008) 273–287.
[3] J.C. Maxwell-Garnett, Colours in metal glasses and in metallic films, Philos. Trans. Roy. Soc. A 203 (1904) 385–420.
[4] D.A.G. Buruggman, Berechnung verschiedener physikalischer konstanten von heterogenen substanzen, I. Dielektrizitatskontanten and Leitfahigkeiten der Mishkorper aus Isotropen Substanzen, Ann. Physik, Leipzig 24 (1935) 636–679.
[5] R.Y. Jou, S.C. Tzeng, Numerical research of natural convective heat transfer enhancement filled with nanofluid in rectangular enclosure, Int. Commun. Heat Mass Transfer 33 (2006) 727–736.
[6] H.F. Oztop, E. Abu-Nada, Numerical study of natural convection in partially heated rectangular enclosure filled with nanofluid, Int. J. Heat Fluid Flow 29 (2008) 1326–1336.
[7] E. Abu Nada, Effects of variable viscosity and thermal conductivity of Al_2O_3–water nanofluid on heat transfer enhancement in natural in natural convection, Int. J. Heat Fluid Flow 30 (2009) 679–690.
[8] B. Ghasemi, S.M. Aminossadati, A. Raisi, Magnetic field effect on natural convection in a nanofluid filled-square enclosure, Int. J. Therm. Sci. 50 (9) (2011) 1748–1756.
[9] E.B. Ogut, Natural convection of water-based nanofluid in an inclined enclosure with a heat source, Int. J. Therm. Sci. 48 (2009) 2063–2073.
[10] M.K. Das, P.S. Ohal, Natural convection heat transfer augmentation in a partially heated and particularly square cavity utilizing nanofluids, Int. J. Numer. Meth. Heat Fluid Flow 19 (1) (2009) 411–431.
[11] S. Kumar, S.K. Parsad, J. Banerjee, Analysis of flow and thermal field in nanofluid using a single phase thermal dispersion model, Appl. Math. Model. 34 (2008) 573–592.
[12] T. Basak, S. Roy, I. Pop, Heat flow analysis for natural convection within trapezoidal enclosures based on heatline concept, Int. J. Heat Mass Transfer 52 (2009) 2471–2483.
[13] Y. Varol, H.F. Oztop, I. Pop, Natural convection in right-angle porous trapezoidal enclosure partially cooled from inclined wall, Int. Commun. Heat Mass Transfer 36 (2009) 6–15.
[14] Y. Varol, H.F. Oztop, I. Pop, Entropy analysis due to conjugate-buoyant flow in right-angle trapezoidal enclosure filled with a porous medium bounded by a solid vertical wall, Int. J. Therm. Sci. 48 (2009) 1161–1175.
[15] Kuang C. Lin, Angela Violi, Natural convection heat transfer of nanofluid in a vertical cavity: effects of non-uniform particle diameter and temperature on thermal conductivity, Int. J. Heat Fluid Flow 31 (2010) 236–245.
[16] H. Saleh, R. Roslan, I. Hashim, Natural convection heat transfer in a nanofluid-filled trapezoidal enclosure, Int. J. Heat Mass Transfer 54 (2011) 194–201.
[17] Seiyed E. Ghasemi, M. Hatami, A. Kalani Sarokolaie, D.D. Ganji, Study on blood flow containing nanoparticles through porous arteries in presence of magnetic field using analytical methods, Physica E 70 (2015) 146–156.
[18] S.E. Ghasemi, M. Hatami, G.H.R. Mehdizadeh Ahangar, D.D. Ganji, Electrohydrodynamic flow analysis in a circular cylindrical conduit using least square method, J. Electrostat. 72 (2014) 47–52.
[19] M. Rahimi-Gorji, O. Pourmehran, M. Hatami, D.D. Ganji, Statistical optimization of microchannel heat sink (MCHS) geometry cooled by different nanofluids using RSM analysis, Eur. Phys. J. Plus (2015) 130–222.
[20] M. Hatami, D.D. Ganji, Thermal behavior of longitudinal convective–radiative porous fins with different section shapes and ceramic materials (SiC and Si3N4), Ceram. Int. 40 (2014) 6765–6775.
[21] Bui Hung Thang, Phan Ngoc Khoi, Phan Ngoc Minh. Minh, A modified model for thermal conductivity of carbon nanotube-nanofluids, Phys. Fluids 27 (3) (2015) 032002 (1994-present).
[22] C. Taylor, P. Hood, A numerical solution of the Navier-Stokes equations using finite element technique, Comput. Fluids 1 (1973) 73–89.
[23] P. Dechaumphai, Finite Element Method in Engineering, second ed., Chulalongkorn University Press, Bangkok, 1999.